Unraveling the magnetic properties of $BiFe_{0.5}Cr_{0.5}O_3$ thin films

G. Vinai, A. Khare, D. S. Rana, E. Di Gennaro, B. Gobaut, R. Moroni, A. Yu. Petrov, U. Scotti di Uccio, G. Rossi, F. Miletto Granozio, G. Panaccione, and P. Torelli

Citation: APL Materials **3**, 116107 (2015); doi: 10.1063/1.4935618

View online: https://doi.org/10.1063/1.4935618

View Table of Contents: http://aip.scitation.org/toc/apm/3/11

Published by the American Institute of Physics

Unraveling the magnetic properties of $BiFe_{0.5}Cr_{0.5}O_3$ thin films

G. Vinai,[1] A. Khare,[2,3] D. S. Rana,[4] E. Di Gennaro,[2] B. Gobaut,[5] R. Moroni,[6] A. Yu. Petrov,[1] U. Scotti di Uccio,[2] G. Rossi,[1,7] F. Miletto Granozio,[2] G. Panaccione,[1] and P. Torelli[1]

[1]*Laboratorio TASC, IOM-CNR, S.S. 14 km 163.5, Basovizza, I-34149 Trieste, Italy*
[2]*CNR-SPIN Napoli and Dipartimento di Fisica, Università di Napoli "Federico II," I-80126 Napoli, Italy*
[3]*Department of Physics, Sungkyunkwan University, Suwon 440 746, South Korea*
[4]*Department of Physics, Indian Institute of Science Education and Research Bhopal, Govindpura, Bhopal 462023, India*
[5]*Sincrotrone Trieste S.C.p.A., S.S. 14 Km 163.5, Area Science Park, 34149 Trieste, Italy*
[6]*CNR-SPIN, Corso Perrone 24, I-16152 Genova, Italy*
[7]*Department of Physics, Università degli Studi di Milano, via Celoria 16, I-20133 Milano, Italy*

(Received 23 June 2015; accepted 2 November 2015; published online 16 November 2015)

We investigate the structural, chemical, and magnetic properties on $BiFe_{0.5}Cr_{0.5}O_3$ (BFCO) thin films grown on (001) (110) and (111) oriented $SrTiO_3$ (STO) substrates by x-ray magnetic circular dichroism and x-ray diffraction. We show how highly pure BFCO films, differently from the theoretically expected ferrimagnetic behavior, present a very weak dichroic signal at Cr and Fe edges, with both moments aligned with the external field. Chemically sensitive hysteresis loops show no hysteretic behavior and no saturation up to 6.8 T. The linear responses are induced by the tilting of the Cr and Fe moments along the applied magnetic field. [http://dx.doi.org/10.1063/1.4935618]

Multiferroic materials (MFs) present both magnetic and ferroelectric orders in the same phase. This property has prompted a renewed interest as, beyond the open physics questions, expectations have been raised on possible applications in functional devices.[1–5]

Bismuth ferrite $BiFeO_3$ (BFO) is the most extensively MF system studied[6,7] as it shows MF properties at room temperature. Bulk BFO is a G-type antiferromagnet with cycloid of 62-64 nm,[8] with a weak ferromagnetic moment induced by the spin canting due to Dzyaloshinskii-Moriya interaction.[9] In recent years, much effort has been dedicated to maximizing the ferromagnetic response of BFO. One approach addressed to achieve this aim is doping BFO with substitutional impurities.[10] An alternative approach is to combine two MF materials, BFO and $BiCrO_3$ (BCO)—the latter being an antiferromagnet with weak ferromagnetic signal at low temperatures.[11–14] This new MF material, $BiFe_{0.5}Cr_{0.5}O_3$ (BFCO), has been theoretically predicted[15,16] to have a double-perovskite structure. The interest of such material is that, if Fe and Cr sublattices are chemically ordered, the expected antiferromagnetic super-exchange coupling[17] between Fe and Cr[18] may yield a ferrimagnetic ordering with a net predicted magnetic moment of 2 μ_B per unit cell.[19] However, the measured values of magnetization are widely spread,[20–27] from nearly zero with antiferromagnetic-like behavior[20,26] to large magnetic moments and magnetic saturation at 0.5 T.[21,22] In the first case, the absence of a strong ferrimagnetic signal has been attributed to the lack of chemical order in the double-perovskite, with Fe and Cr atoms being randomly distributed.[26] All the reported hysteresis loops of BFCO thin films have been measured by integrating methods, like vibrating sample magnetometers,[22,23] SQUID,[21,25,26] or alternating gradient magnetometer.[24] In this article, we exploited the chemical sensitivity of x-ray magnetic circular dichroism (XMCD) at Fe and Cr $L_{2,3}$ edges to perform a systematic study of the BFCO magnetic properties. The first merit of such a technique is the chemical sensitivity of the magnetic measurement, which allows to directly address

the magnetic order of the Cr and Fe sublattices and to exclude possible spurious contribution to the magnetization signal. In fact, it has been clearly demonstrated that in BFO thin films, the presence of secondary ferrimagnetic phases of γ-Fe_2O_3 is the main responsible of the magnetic signal that otherwise tends to zero for high purity films.[28] In this study, the presence of secondary phases is carefully evaluated by x-ray absorption spectroscopy (XAS) and x-ray diffraction (XRD). The second unique merit of this method is that, by comparing the XMCD spectra of Fe and Cr, it is possible to verify the hypothesis of a magnetic configuration characterized by a ferromagnetic in-plane alignment of similar cations and an antiferromagnetic alignment of different cations.[15,19] Indeed, in presence of the predicted chemically and magnetically ordered unit cell, the Cr and Fe planes in the BFCO structure would provide large dichroic signals with opposite signs. The unbalance of the atomic moments of the two cations would lead to a clear ferrimagnetic behavior.

In this paper, we show how highly pure BFCO thin films do not display any signature of ferrimagnetic behavior. In fact, no hysteretic behavior and no remanence are found at the Cr and Fe edges and no saturation is achieved even at the highest applied field. This result shows that Cr and Fe moments tilt in the direction of the applied magnetic field, even in the presence of some degree of Cr-Fe chemical order.

$SrRuO_3$-buffered epitaxial BFCO thin films (thicknesses ~30 nm) were grown at the Indian Institute of Science Education and Research by pulsed laser deposition (PLD) on (001), (110), and (111)-oriented $SrTiO_3$ (STO) single crystal. A KrF excimer laser (wavelength = 248 nm) was focused to reach an energy density of 2 J/cm^2 with a repetition rate of 4 Hz on the target surface. A ceramic target of $Bi_{2.2}FeCrO_6$, selected on purpose with a 10% Bi excess to compensate for the high volatility of Bi, was used for depositing the BFCO films. The 20 nm thick $SrRuO_3$ (SRO) bottom electrode was grown on all substrates at 700 °C at an oxygen partial pressure (OPP) of 50 Pa prior to BFCO deposition. BFCO films were then deposited at 750 °C on OPP of 1.1 Pa. After deposition, the films were cooled from 750 °C down to 500 °C in OPP of 100 Pa and hold for 1 h at this temperature to guarantee full oxidation, prior to cooling to room temperature.

The structure of the as-grown films was characterized by high resolution x-ray diffraction (HR-XRD) technique (PANalytical's EMPYREAN) with Cu-K_α radiation. Rocking curves (ω-scan) were used to determine the epitaxial quality, whereas in-plane Φ scans were performed to check the epitaxial relationship between the substrate and thin films.[29]

XAS and XMCD measurements were performed on the EPFL/PSI X-Treme beamline at the Swiss Light Source, Paul Scherrer Institut, Villigen, Switzerland[30] and at Advanced Photoelectric Effect (APE) beamline of IOM-CNR at the Elettra synchrotron radiation facility.[31] At the X-Treme beamline, the samples were measured at 2 K temperature with an applied magnetic field of ±6.8 T oriented along the x-ray beam direction; the direction of the magnetic field with respect to the sample was varied by rotating the sample with respect to the circularly polarized x-ray beam. XMCD measurements were performed at Cr and Fe $L_{2,3}$ edges in total electron yield detection mode, by alternating the x-ray beam helicity under the applied magnetic field. Chemically sensitive hysteresis loops on both Cr and Fe edges were also measured at 2 K, scanning the magnitude of the magnetic field in the range ±6.8 T, by selecting L_3 edge and pre-edge absorption spectra of each element and switching the photon helicity. At the APE beamline, XAS and XMCD measurements were done in total electron yield and fluorescence yield detection modes at 80 K temperature with a magnetic pulse of ±0.05 T parallel to the sample surface.

HR-XRD analysis shows good epitaxy of all BFCO films of different orientations. θ-2θ scans show peaks consistent with single-phase, perovskite-like, pseudo-cubic films. Furthermore, no recognizable signs of impurity phases are detected within the instrumental detection limit. In the θ-2θ scans, peaks corresponding to a double periodicity are visible on (111) samples. This is consistent with some degree of chemical ordering of Fe and Cr on alternating (111) planes.[23] The rocking curve (ω-scan) and in-plane Φ scans confirm the epitaxial growth and the excellent crystallinity of the films. Detailed description of the structural analysis is presented in the supplementary material.[32]

Figure 1 shows the XAS spectra at Cr and Fe $L_{2,3}$ edges for the sample BFCO/SRO/STO (001) at grazing incidence (60° with respect to the normal of the sample surface). The spectra are the average of the two opposite helicities. Curves have been normalized by subtracting the constant background signal to zero and normalizing to one, the highest intensity of the signal (i.e., the L_3 edge).

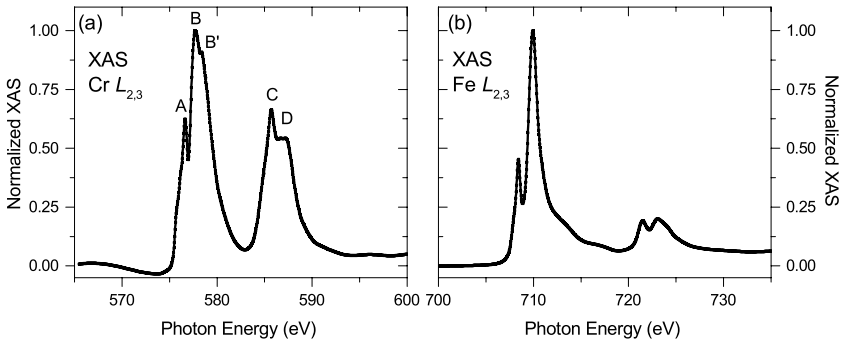

FIG. 1. XAS spectra at Cr (a) and Fe (b) $L_{2,3}$ edges on BFCO/SRO/STO (001) sample at grazing incidence with 6.8 T applied magnetic field. For Cr spectra, splitting structures are labeled.

Both Cr and Fe present a valence of 3+. The Cr^{3+} spectrum is consistent with octahedral symmetry, with $(t_{2g})^3$ ground state; its crystal field splitting structures (in Figure 1(a), peaks labeled A and C for e structures and B, B′, and D for t_2 structures) are close to those simulated for Cr_2O_3.[33] Also Fe^{3+} presents octahedral symmetry,[34] in good agreement with what observed on Fe edge spectra in BFO thin films.[28] The 3+ octahedral ground state is consistent with expectation from theoretical models.[15,16] The same XAS features at both Cr and Fe edges were observed for all the three crystallographic orientations.

In Figure 2, we present the XMCD spectra at grazing incidence, with an applied magnetic field of 6.8 T, at Cr and Fe $L_{2,3}$ edges for STO substrates with crystalline orientation (001) (black line), (110) (red line), and (111) (blue line). We notice that the shape of the dichroic signal at the Cr edge is in agreement with the one of octahedral Cr^{3+} in other compounds,[35,37,38] as shown in the figure;

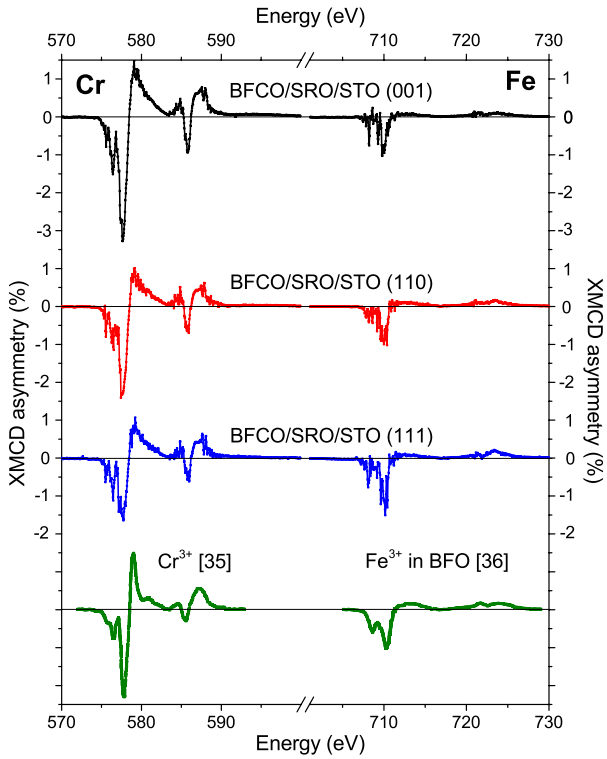

FIG. 2. XMCD spectra at Cr and Fe $L_{2,3}$ edges with 6.8 T applied magnetic field at grazing incidence on BFCO samples with STO (001) (black line), (110) (red line), and (111) (blue line) substrates, compared with the XMCD spectra of Cr^{3+}[35] and Fe^{3+} in BFO[36] (green line).

the dichroic signal at the Fe edge does not show the negative peaks of the Fe^{2+} and Fe^{3+} octahedral sites, separated by the positive peak of the Fe^{3+} tetrahedral site, typical of γ-Fe_2O_3.[28,39] Indeed, the shape of Fe XMCD strongly resembles the one extrapolated for a pure BFO thin film by removing the γ-Fe_2O_3 contribution from Fe spectra obtained for $BiFe_{0.85}Co_{0.15}O_3$ in Ref. 36, as shown at the bottom of Figure 2, confirming the quality of the primary phase in BFCO.

Contrary to the behavior expected for a system showing the foreseen spin configuration, both Cr and Fe magnetic moments align with the field direction in all samples. Looking at the intensity of the dichroic signal at 6.8 T, the three samples show different values at the Cr peak: 3.3% for STO (001), 2.3% for STO (110), and 1.6% for STO (111), respectively. By applying the sum rules,[40] the correspondingly total magnetic moments are, respectively, 0.11 ± 0.04, 0.1 ± 0.04, and 0.04 ± 0.06 μ_B/Cr. The large error bars take into account the incertitude coming from the partial overlapping of L_2 and L_3 edges on Cr spectra while for the Fe (where separation between of L_2 and L_3 is large enough), the error bar accounts basically for the small magnitude of the dichroic signal, which is close to 1% for all samples. Here, the error bars for the sum rule analysis are too large to extract reliable values of total magnetic moment. However, by making an evaluation of the Fe moment based on the magnitude of the XMCD asymmetry, it is possible to extrapolate values of BFCO total net moment, resulting from the sum of Fe and Cr contributions, in the range from 0.08 to 0.15 ± 0.06 μ_B per unit cell. These values are comparable with those obtained by magnetometric measurements in BFCO thin films with weak ferromagnetic behavior.[20,26,29]

Similar measurements as in Figure 2 were repeated with the magnetic field oriented perpendicularly with respect to the sample surface, as shown in the supplementary material.[32] Also in this latter case, the magnetization of both Cr and Fe is oriented parallel to the field. The intensity of the dichroic signals slightly changes according to the direction of the applied magnetic field with respect to the sample surface. By combining this result with those obtained from Figure 2, we observe that the relative intensity of the XMCD asymmetries changes both as a function of the direction of the applied magnetic field and of BFCO different crystallographic orientations, the sign of the anisotropic behavior of the samples.

In order to observe the response of Cr and Fe atoms in a wide range of applied magnetic field, chemically sensitive hysteresis loops have been performed on the two edges at grazing incidence, with magnetic field up to 6.8 T. The hysteresis loops of the sample BFCO/SRO/STO (001) are shown in Figure 3.

The magnetization curve at Cr edge shows an increase of the dichroic response with increasing magnetic field, without reaching the magnetic saturation at highest available fields. No hysteretic behavior is detected. In the case of Fe edge, the intensity of the magnetic response is even smaller,

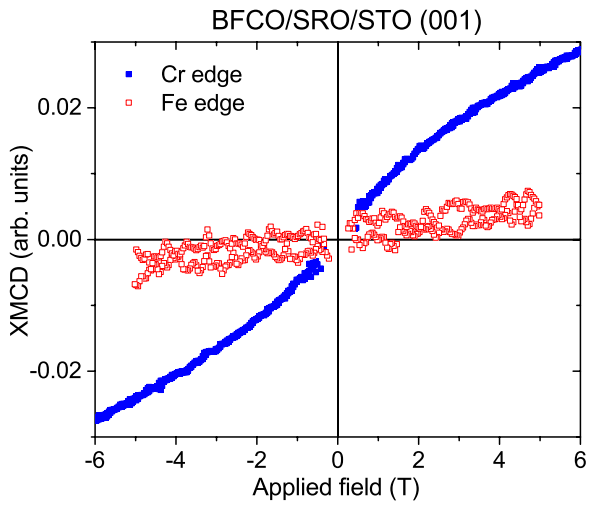

FIG. 3. Chemically sensitive hysteresis loops at Cr (blue dots) and Fe (red dots) edges for BFCO/SRO/STO (001) sample at grazing incidence. Because of the experimental setup, noise at low fields was larger than the signal of the sample; thus, those points have been removed.

consistently with the XMCD scans at 6.8 T. Also in this case, no clear magnetic saturation is observed and the resolution of the measurement does not permit to detect a hysteretic behavior. The samples with different crystallographic orientations both showed similar hysteresis curves with paramagnetic-like behavior (i.e., no remanence, no hysteretic behavior, and linear response). Consistently with what observed with XMCD spectra, both Cr and Fe edges follow the applied magnetic field in the same direction. Concerning the behavior at low fields, XMCD measurements performed at 80 K after magnetic pulses of 0.05 T showed no dichroic signal at either Cr or Fe edges for both total electron yield and fluorescence yield measurements. From these combined measurements, we can conclude that Cr and Fe edges present no remanence at low temperatures. These features were observed on all three crystallographic orientations at both Cr and Fe edges.

In summary, the predicted ferrimagnetic order[15,16,19] is not confirmed by our measurements that show a good crystalline order with some degree of chemical ordering (see the supplementary material[32]) but a lack of ferrimagnetic order (the signs of XMCD of Fe and Cr are parallel) and a very low intensity of the net moments of each element. The dichroic signal measured at Cr and Fe edges is thus attributed to the tilting of the spins in the direction of the applied magnetic field, with the resulting net moment increasing for increasing magnetic fields, as observed in the paramagnetic-like hysteresis loops.

It is possible to give an evaluation of the tilting angle of Cr and Fe moments under the applied magnetic field. As a case of study, we consider the case of BFCO/SRO/STO (111) sample and magnetic field applied perpendicularly to the sample surface, whose XMCD spectra at Cr and Fe edges are shown in the supplementary material.[32] In this configuration, the plane on which the Fe and Cr spins are lying is normal to the applied magnetic field;[41] thus, the measured dichroic signals are the projection of the Cr and Fe moments on the magnetic hard axis. By applying the sum rules, in this configuration, BFCO/SRO/STO (111) sample presents at 2 K under 6.8 T magnetic field a spin moment of $0.07 \pm 0.08\ \mu_B$ for Cr and $0.03 \pm 0.08\ \mu_B$ for Fe. By considering the atomic spin moments of Cr and Fe *B* cations, with corresponding values of 3 μ_B and 5 μ_B, respectively, we obtain a tilting of 1.3° for Cr and 0.4° for Fe moments. From these tilting values, an estimation of the exchange coupling can be given by modeling the total energy through a Heisenberg Hamiltonian.[42–45] By considering a minimal Heisenberg Hamiltonian with nearest neighbor interactions under an applied magnetic field,[46] we can define

$$H = -J \sum_{i,j} \vec{S}_i \cdot \vec{S}_j - 2\mu_B \left(\sum_{i(Fe)} \vec{S}_{i(Fe)} \cdot \vec{H} + \sum_{i(Cr)} \vec{S}_{i(Cr)} \cdot \vec{H} \right) \quad (1)$$

with $\vec{H}$ being the applied magnetic field vector and $\vec{S}_{(Cr)}$ and $\vec{S}_{(Fe)}$ the atomic spin moments of Cr and Fe *B* cations. If among all the possible spin interactions we take into account only the Cr-Fe one, we obtain a value of exchange coupling of −0.4 meV, in good agreement with the theoretical models.[15,19]

Finally, concerning the imbalance between Cr and Fe spectra in the intensity of dichroic signals, we attribute it either to the different anisotropic responses of octahedral Fe and Cr elements, which may be due to the differences of the distances of the surrounding atoms in the respective subcells, or to the different strengths of the Cr-Cr or Fe-Fe couplings. The intensity of the discrepancy appears to be dependent on BFCO crystalline orientation, as it can be observed in Figure 2, with a maximum difference in Cr and Fe dichroic signal intensities for the (001) crystallographic orientation and a minimum one for the (111) orientation.

In this article, we have reported an element-specific study addressing the magnetic properties of highly pure BFCO thin films, epitaxially grown on SRO-buffered STO substrates with three different crystallographic orientations: (001), (110), and (111). XMCD measurements performed at 2 K under 6.8 T magnetic field show Cr and Fe net magnetic moments far below those predicted for a ferrimagnetic, *B*-site ordered BFCO layered perovskite. Cr and Fe moments appear to be both aligned with the external field. The maximum total magnetic moment measured has a value of 0.15 μ_B per unit cell, recorded at grazing incidence for (001) surface. Chemically sensitive hysteresis loops show a paramagnetic-like response of both Cr and Fe, with no hysteretic behavior

and remanence close to zero. The dichroic signal at 6.8 T is due to the tilting of Cr and Fe moments toward the direction of the applied magnetic field.

This work was partly funded by the Italian Ministry of Research through the project PRIN "Interfacce di ossidi: nuove proprietà emergenti, multifunzionalità e dispositivi per l'elettronica e l'energia (OXIDE)" and through the NFFA project. G.V. thanks S. Rusponi, C. Piamonteze, and F. Telesio for the support during the beamtime at SLS. The research leading to these results has received funding from the European Community's Seventh Framework Programme (No. FP7/2007-2013) under Grant Agreement No. 312284 (CALIPSO). D.S.R. thankfully acknowledges the financial support from SERB-DST, New Delhi in the form of research Project No. SR/S2/LOP-0013/2010.

[1] S. Fusil, V. Garcia, A. Barthélémy, and M. Bibes, Annu. Rev. Mater. Res. **44**, 91 (2014).
[2] J. Ma, J. Hu, Z. Li, and C. W. Nan, Adv. Mater. **23**, 1062 (2011).
[3] L. W. Martin and R. Ramesh, Acta Mater. **60**, 2449 (2012).
[4] N. A. Hill, J. Phys. Chem. B **104**, 6694 (2000).
[5] N. A. Hill and A. Filippetti, J. Magn. Magn. Mater. **242-245**, 976 (2002).
[6] G. Catalan and J. F. Scott, Adv. Mater. **21**, 2463 (2009).
[7] J.-G. Park, M. D. Le, J. Jeong, and S. Lee, J. Phys.: Condens. Matter **26**, 433202 (2014).
[8] I. Sosnowska, T. P. Neumaier, and E. Steichele, J. Phys. C: Solid State Phys. **15**, 4835 (1982).
[9] C. Ederer and C. J. Fennie, J. Phys.: Condens. Matter **20**, 434219 (2008).
[10] H. Ishiwara, Curr. Appl. Phys. **12**, 603 (2012).
[11] A. A. Belik, J. Solid State Chem. **195**, 32 (2012).
[12] S. Niitaka, M. Azuma, M. Takano, E. Nishibori, M. Takata, and M. Sakata, Solid State Ionics **172**, 557 (2004).
[13] M. Murakami, S. Fujino, S. H. Lim, C. J. Long, L. G. Salamanca-Riba, M. Wuttig, I. Takeuchi, V. Nagarajan, and A. Varatharajan, Appl. Phys. Lett. **88**, 152902 (2006).
[14] M. Opel, E. P. Menzel, A. Nielsen, D. Reisinger, K. W. Nielsen, A. Brandlmaier, F. D. Czeschka, M. Althammer, M. Weiler, S. T. B. Goennenwein, J. Simon, M. Svete, W. Yu, S. M. Hühne, W. Mader, R. Gross, and S. Geprags, Phys. Status Solidi **208**, 232 (2011).
[15] P. Baettig, C. Ederer, and N. A. Spaldin, Phys. Rev. B **72**, 214105 (2005).
[16] P. Baettig and N. A. Spaldin, Appl. Phys. Lett. **86**, 012505 (2005).
[17] P. W. Anderson, Phys. Rev. **115**, 2 (1959).
[18] A. S. Moskvin, N. S. Ovanesyan, and V. A. Trukhtanov, Hyperfine Interact. **1**, 265 (1975).
[19] M. Goffinet, J. Íñiguez, and P. Ghosez, Phys. Rev. B **86**, 024415 (2012).
[20] D. H. Kim, H. N. Lee, M. D. Biegalski, and H. M. Christen, Appl. Phys. Lett. **91**, 042906 (2007).
[21] N. Ichikawa, M. Arai, Y. Imai, K. Hagiwara, H. Sakama, M. Azuma, Y. Shimakawa, M. Takano, Y. Kotaka, M. Yonetani, H. Fujisawa, M. Shimizu, K. Ishikawa, and Y. Cho, Appl. Phys. Express **1**, 101302 (2008).
[22] R. Nechache, C. Harnagea, L. P. Carignan, O. Gautreau, L. Pintilie, M. P. Singh, D. Ḿnard, P. Fournier, M. Alexe, and A. Pignolet, J. Appl. Phys. **105**, 061621 (2009).
[23] B. Aïssa, R. Nechache, D. Therriault, F. Rosei, and M. Nedil, Appl. Phys. Lett. **99**, 183505 (2011).
[24] L. Sha, J. Miao, S. Z. Wu, X. G. Xu, Y. Jiang, and L. J. Qiao, J. Alloys Compd. **554**, 299 (2013).
[25] M. R. Suchomel, C. I. Thomas, M. Allix, M. J. Rosseinsky, A. M. Fogg, and M. F. Thomas, Appl. Phys. Lett. **90**, 112909 (2007).
[26] V. Shabadi, M. Major, P. Komissinskiy, M. Vafaee, A. Radetinac, M. Baghaie yazdi, W. Donner, and L. Alff, J. Appl. Phys. **116**, 114901 (2014).
[27] R. Nechache, C. Nauenheim, U. Lanke, A. Pignolet, F. Rosei, and A. Ruediger, J. Phys.: Condens. Matter **24**, 142202 (2012).
[28] H. Béa, M. Bibes, S. Fusil, K. Bouzehouane, E. Jacquet, K. Rode, P. Bencok, and A. Barthélémy, Phys. Rev. B **74**, 020101(R) (2006).
[29] A. Khare, A. Singh, S. S. Prabhu, and D. S. Rana, Appl. Phys. Lett. **102**, 192911 (2013).
[30] C. Piamonteze, U. Flechsig, S. Rusponi, J. Dreiser, J. Heidler, M. Schmidt, R. Wetter, M. Calvi, T. Schmidt, H. Pruchova, J. Krempasky, C. Quitmann, H. Brune, and F. Nolting, J. Synchrotron Radiat. **19**, 661 (2012).
[31] G. Panaccione, I. Vobornik, J. Fujii, D. Krizmancic, E. Annese, L. Giovanelli, F. Maccherozzi, F. Salvador, A. De Luisa, D. Benedetti, A. Gruden, P. Bertoch, F. Polack, D. Cocco, G. Sostero, B. Diviacco, M. Hochstrasser, U. Maier, D. Pescia, C. H. Back, T. Greber, J. Osterwalder, M. Galaktionov, M. Sancrotti, and G. Rossi, Rev. Sci. Instrum. **80**, 043105 (2009).
[32] See supplementary material at http://dx.doi.org/10.1063/1.4935618 for a detailed description of the XRD characterization (θ-2θ scans, superstructure peaks, rocking curves and Φ scans), for the comparison between XMCD measurements at grazing and normal incidence and a discussion on the sum analysis method on our samples.
[33] C. Theil, J. van Elp, and F. Folkmann, Phys. Rev. B **59**, 7931 (1999).
[34] J. P. Crocombette, M. Pollak, F. Jollet, N. Thromat, and M. Gautier-Soyer, Phys. Rev. B **52**, 3143 (1995).
[35] N. D. Telling, V. S. Coker, R. S. Cutting, G. Van Der Laan, C. I. Pearce, R. A. D. Pattrick, E. Arenholz, and J. R. Lloyd, Appl. Phys. Lett. **95**, 163701 (2009).
[36] V. R. Singh, V. K. Verma, K. Ishigami, G. Shibata, Y. Yamazaki, A. Fujimori, Y. Takeda, T. Okane, Y. Saitoh, H. Yamagami, Y. Nakamura, M. Azuma, and Y. Shimakawa, J. Appl. Phys. **114**, 103905 (2013).
[37] S. W. Han, J.-S. Kang, S. S. Lee, G. Kim, S. J. Kim, C. S. Kim, J.-Y. Kim, H. J. Shin, K. H. Kim, J. I. Jeong, B.-G. Park, J.-H. Park, and B. I. Min, J. Phys. Condens. Matter **18**, 7413 (2006).

[38] G. van der Laan, R. V. Chopdekar, Y. Suzuki, and E. Arenholz, Phys. Rev. Lett. **105**, 067405 (2010).
[39] S. Brice-Profeta, M.-A. Arrio, E. Tronc, N. Menguy, I. Letard, C. Cartier dit Moulin, M. Noguès, C. Chanéac, J.-P. Jolivet, and P. Sainctavit, J. Magn. Magn. Mater. **288**, 354 (2005); S. Brice-Profeta, M. A. Arrio, E. Tronc, I. Letard, C. C. D. Moulin, and P. Sainctavit, Phys. Scr. **T115**, 626 (2005).
[40] C. T. Chen, Y. U. Idzerda, H.-J. Lin, N. V. Smith, G. Meigs, E. Chaban, G. H. Ho, E. Pellegrin, and F. Sette, Phys. Rev. Lett. **75**, 152 (1995).
[41] B. Ruette, S. Zvyagin, A. Pyatakov, A. Bush, J. Li, V. Belotelov, A. Zvezdin, and D. Viehland, Phys. Rev. B **69**, 064114 (2004).
[42] I. Sosnowska and A. K. Zvezdin, J. Magn. Magn. Mater. **140-144**, 167 (1995).
[43] M. Matsuda, R. S. Fishman, T. Hong, C. H. Lee, T. Ushiyama, Y. Yanagisawa, Y. Tomioka, and T. Ito, Phys. Rev. Lett. **109**, 067205 (2012).
[44] U. Nagel, R. S. Fishman, T. Katuwal, H. Engelkamp, D. Talbayev, H. T. Yi, S. W. Cheong, and T. Rõõm, Phys. Rev. Lett. **110**, 257201 (2013).
[45] J. Jeong, E. A. Goremychkin, T. Guidi, K. Nakajima, G. S. Jeon, S. A. Kim, S. Furukawa, Y. B. Kim, S. Lee, V. Kiryukhin, S. W. Cheong, and J. G. Park, Phys. Rev. Lett. **108**, 077202 (2012).
[46] J. C. Bonner and M. E. Fisher, Phys. Rev. **135**, A640 (1964).